THE JOURNAL OF BIOLOGICAL CHEMISTRY VOL. 289, NO. 8, pp. 4980–4988, February 21, 2014

A Novel Endosomal Sorting Complex Required for Transport (ESCRT) Component in *Arabidopsis thaliana* Controls Cell Expansion and Development*

Received for publication, October 23, 2013, and in revised form, December 26, 2013 Published, JBC Papers in Press, January 2, 2014, DOI 10.1074/jbc.M113.529685

Francisca C. Reyes[‡§], Rafael A. Buono[‡], Hannetz Roschzttardtz[‡], Simone Di Rubbo[¶‖], Li Huey Yeun[‡], Eugenia Russinova[¶‖], and Marisa S. Otegui[‡1]**

*From the [‡]Department of Botany, University of Wisconsin-Madison, Madison, Wisconsin 53706, the [§]Centro de Biotecnologia Vegetal, Universidad Andrés Bello, Republica 217 Santiago 8370146, Chile, the [¶]Department of Plant Systems Biology, VIB, and Ghent University, 9052 Ghent, Belgium, the [‖]Department of Plant Biotechnology and Bioinformatics, Ghent University, 9052 Ghent, Belgium, and the **Department of Genetics, University of Wisconsin-Madison, Madison, Wisconsin 53706*

Background: ESCRT mediates membrane remodeling in cellular processes such as endosomal sorting. The ATPase SKD1/VPS4 is essential for ESCRT function.
Results: PROS is a plant-specific ESCRT component that increases SKD1/VPS4 ATPase activity and is required for cell expansion.
Conclusion: Plants have evolved specific ESCRT components that are required for normal development.
Significance: Diversification of ESCRT components in eukaryotes may provide additional regulatory mechanisms for ESCRT-dependent processes.

ESCRT proteins mediate membrane remodeling and scission events and are essential for endosomal sorting of plasma membrane proteins for degradation. We have identified a novel, plant-specific ESCRT component called PROS (POSITIVE REGULATOR OF SKD1) in *Arabidopsis thaliana*. PROS has a strong positive effect on the *in vitro* ATPase activity of SKD1 (also known as Vacuolar Protein Sorting 4 or VPS4), a critical component required for ESCRT-III disassembly and endosomal vesiculation. PROS interacts with both SKD1 and the SKD1-positive regulator LIP5/VTA1. We have identified a putative MIM domain within PROS that mediate the interaction with the MIT domain of SKD1. Interestingly, whereas MIM domains are commonly found at the C terminus of ESCRT-III subunits, the PROS MIM domain is internal. The heterologous expression of *PROS* in yeast mutant cells lacking Vta1p partially rescues endosomal sorting defects. PROS is expressed in most tissues and cells types in *Arabidopsis thaliana*. Silencing of PROS leads to reduced cell expansion and abnormal organ growth.

Endosomal sorting of signaling receptors, transporters, and other plasma membrane proteins is a key process that controls plasma membrane protein composition and therefore, the ability of cells to respond to extracellular stimuli. Plasma membrane proteins are continuously internalized by endocytosis and delivered to endosomes. At the endosomal membranes, the endosomal sorting complex required for transport (ESCRT)[2] bind and concentrate the ubiquitinated cargo and mediate their sorting into intraluminal vesicles, giving rise to multivesicular bodies (MVB). In fungi and metazoans, ESCRT-0, I, and II are assumed to recognize and concentrate the cargo proteins while initiating or stabilizing negative membrane curvature on the endosomal membrane. ESCRT-III polymerizes into long filaments and drives membrane deformation, constriction, and membrane scission *in vitro* (1–5). Finally, the AAA ATPase SKD1/Vps4p (Suppressor of K^+ Transport Growth Defect 1/Vacuolar Protein Sorting 4) together with its cofactor LIP5/Vta1p disassemble and recycle the ESCRT coats back to the cytoplasm (6).

There are four core ESCRT-III subunits, Vps20p/CHMP6, Snf7p/CHMP4, Vps24p/CHMP3, and Vps2p/CHMP2 (with several isoforms in animal and plants) and three accessory subunits Did2p/CHMP1 (7, 8), Vps60p/CHMP5 (9–11), and IST1 (12, 13). The three first core subunits are sufficient for driving membrane scission *in vitro* (3) whereas Vps2p recruits the Vps4p/SKD1 complex to the endosomal membrane (14). The accessory ESCRT-III subunits play a modulatory effect on Vps4p/SKD1function (7, 12).

ESCRT proteins are ancient components of the eukaryotic endomembrane machinery and are found in all five major groups of eukaryotes (15). Plants contain orthologs for most of the ESCRT-I to III proteins identified in metazoans and fungi (15, 16) but they also have undergone a significant diversification, exhibiting multiple isoforms of most ESCRT components (17–22).

* This work was supported by NSF Grant MCB1157824 (to M. S. O.) and by the Marie-Curie Initial Training Network Bravissimo (PITN-GA-2008-215118; to E. R. and S. D. R.).
[1] To whom correspondence should be addressed: B119, Birge Hall, 430 Lincoln Drive, Madison, WI 53706. Tel.: 608-265-5703; Fax: 608-262-7509; E-mail: otegui@wisc.edu.

[2] The abbreviations used are: ESCRT, endosomal sorting complex required for transport; MVB, multivesicular body; BiFC, bimolecular fluorescence complementation; GUS, β-glucuronidase; MIM, MIT-interacting motif; MIT, microtubule interacting and transport; PROS, positive regulator of SKD1; SKD1/Vps4p, suppressor of K+ transport growth defect 1/vacuolar protein sorting 4.

Here, we characterized a novel ESCRT component found in plants called PROS (POSITIVE REGULATOR OF SKD1). PROS interacts with *Arabidopsis* SKD1 and LIP5 and is able to induce a strong increase in the *in vitro* ATPase activity of both plant SKD1 and yeast Vps4p. Plants with reduced levels of *PROS* transcripts were dwarf and showed cell expansion and organ formation defects, indicating that PROS plays a key role on plant development.

EXPERIMENTAL PROCEDURES

Protein Purification and Interaction Assays—Recombinant proteins were expressed in *Escherichia coli* BL21. The cDNA fragments were cloned either in pGEX (GE Healthcare Life Sciences), pET or both using the restriction sites BamHI and *EcoR*I for all of them except for *IST1* that was cloned between the SalI and NotI sites, to generate N terminus GST- or His_6- fusion proteins. *PROS* and *CHMP1A* were amplified from the ABRC clones U11633 and U16228, respectively. *VPS60.1* and *IST1* were amplified from Col-0 WT cDNA; *SKD1* was amplified using the clone described in (20) as a template. For the GST alone control, the pGEX vector was used. GST-fusion proteins were purified using glutathione-agarose beads (Sigma-Aldrich) and His_6-fusion proteins were purified using Ni-NTA (nickel nitrilotriacetic acid)-agarose beads (Qiagen). Mutations in PROS (A1, A2, A3) and SKD1 (L63A) were introduced by PCR. Expression of His-SKD1, His-LIP5 (20); His-CHMP1A (19); His-Vta1p (23) and His-Vps4p (24) was performed as previously described. For the *in vitro* interaction pull-down experiments, equivalent amounts of the purified proteins were incubated 2 h at 4 °C in 20 mM Hepes, pH 7.4, 300 mM NaCl, 5 mM $MgCl_2$, 10% (v/v) glycerol, and 0.02% (v/v) Nonidet P-40 (Input). The glutathione-agarose beads were then rinsed three times with the same buffer described above except that 0.2% (v/v) of Nonidet P-40 was used (Output). Both samples were denatured using Laemmli buffer, separated by SDS-PAGE and transferred onto nitrocellulose membrane. The proteins were detected using anti-His_6 antibodies (Sigma) and anti-GST antibody (19).

Yeast Two-hybrid Assay—PROS and *SKD1* cDNAs were cloned in-frame with the GAL4 DNA binding domain (BD) in the vector pBD-GAL4 and with the GAL4 DNA activation domain (AD) of the vector pAD-GAL4 (Stratagene), respectively. The yeast strain AH109 was sequentially transformed with the two vectors according to the manufacturer's protocol. The transformed cells were selected on synthetic dropout (SD) plates lacking Leu and Trp (SD-LW). The expression of *HIS3* and *ADE2* was assessed on plates lacking Leu, Trp, His, and Ade (SD-LWHA).

SKD1 Pull-down from Plant Extracts— 60 mg of 3-week-old rosette leaves were ground in liquid nitrogen and suspended in 500 μl of buffer C (50 mM Tris-HCl pH 7.5, 150 mM NaCl, 0.2% Nonidet P-40). The extract was incubated on ice for 15 min and centrifuged for 10 min at 10.000 $\times$ *g*. Pellet was discarded, and the protein content was quantified; 800 μg of total plant protein were used to test the interaction. GST or PROS-GST bound to glutathione-agarose beads were added to the protein extract and incubated for 2 h at 4 °C in an end-over-end mixer. The mix was centrifuged, and 450 μl of the supernatant were discarded. The remaining 50 μl were homogenized; then, 25 μl were removed (input), and the rest was rinsed three times in buffer C and resuspended in 25 μl of buffer C. The samples were denatured using Laemmli buffer, separated by SDS-PAGE, and transferred onto nitrocellulose membrane. Proteins were detected using anti-SKD1 (20) and anti-GST antibodies (19).

Bifluorescence Complementation (BiFC) Assay—PROS and *SKD1* were cloned in the pSY738 and pSY736 vectors (25). To produce a translational fusion between the N-terminal portion of YFP and PROS (YN-PROS), the open reading frame of *PROS* was PCR-amplified from the ABRC clone U11633. For the expression of SKD1 fused to the C-terminal portion of YFP (SKD1-YC) the open reading frame of *SKD1* was amplified from the clone U12244 (ABRC) using forward and reverse primers containing the restriction sites SalI and NotI, respectively, and cloned into the pSY738 vector. Both vectors were used to transfect protoplasts from 23-day-old seedlings as previously described (26). Approximately 2×10^5 protoplasts were transfected with 10 μg of each vector, and then incubated for 16 h. Empty vectors were used as negative controls, and a vector containing a ^{35}*Sprom::CFP* (pAVA574) reporter (27) was co-transfected to assess transfection efficiency. To analyze interactions, YFP and CFP fluorescence were detected using a Zeiss LSM 510 META confocal laser scanning microscope and a 10× NA0.3 objective. YFP was excited with an Argon laser at 514 nm, 15% of intensity, and the emission was collected using a BP 535-590 IR filter and pinhole opening equivalent to 1 Airy unit. CFP was excited with an Argon laser at 458 nm, 20% of intensity, and the emission was collected using a BP 480–520 IR filter and pinhole opening equivalent to 1 Airy unit. With the aid of Fiji (28), 280–580 protoplasts for each vector combination were scored for CFP fluorescence and reconstitution of YFP fluorescence. The experiment was repeated three times.

ATPase Assay—For the *in vitro* ATPase assays, 2 μM His-SKD1, His-PROS, His-LIP5, His-CHMP1A, His-CHMP1(MIM), His-Vps4p, and His-Vta1p were used for the assay. ATPase activity was measured using a modified malachite green-based colorimetric method (20).

Expression of PROS and Sorting Defect Analysis in Yeast—The *His-PROS* fragment was PCR-amplified from the pET-*His-PROS* vector and cloned into the yeast expression vector pGPD416 using the EcoRI and HindIII sites. *Saccharomyces cerevisiae* strain BY4742 (*MATα, his3Δ1 leu2Δ0 lys2Δ0 ura3Δ0*), Δ*vta1/ΔG418* and Δ*vps4* were kindly donated by David Katzmann, Mayo Clinic-Minnesota. The different yeast strains were transformed with the URA plasmids pGPD416-*His-PROS* or pGPD416-*His-Vta1* and/or the LEU plasmid pRS425-*CPS-GFP* and were grown at 30 °C in liquid medium containing 0.67% (w/v) yeast nitrogen base, 2% (w/v) glucose and synthetic complete media (SCM)-LEU or SCM-URA-LEU. Transformation was performed using lithium acetate, followed by standard procedures. Yeast RNA was isolated using TRIzol (Invitrogen) following the manufacturer's instructions and the retro transcriptase (RT) reaction was performed using oligo-dT primers and AMV-Reverse Transcriptase (Promega).

Living cells were imaged using a Zeiss 510 laser scanning confocal microscope and a 63× oil-immersion NA1.4 objective. GFP was excited with an Argon laser at 488 nm, 20% of intensity, and the emission was collected using a BP 500–530 IR filter and pinhole opening equivalent to 1 Airy unit. All cells with detectable signal in the vacuolar lumen were scored as wild type (WT). The experiment was designed as a blind study. Number-coded cultures containing the eight different yeast strains were placed on glass slides. Between 25 and 30 randomly selected field of views were recorded at three different Z-positions. All cells contained in these images were scored either as mutant or WT for GFP-CPS sorting. The three Z-views were used to determine the localization of the GFP signal either at the vacuolar membrane or the vacuolar lumen. After the quantitative analysis was performed, the data from the number-coded cultures was assign to the eight yeast strains. The experiment was repeated five times with independently transformed yeast cultures.

Generation of Transgenic Plants—Artificial microRNAs (amiRNA) were designed using the Web microRNA designer (WMD2) tool and the amiRNAs were cloned as described in (29). Two amiRNA were used, the first one against the coding region (A) TATCTAAGTAATCGGAAGGAG and the second one against the 3′-UTR (B) TATATATCTACGAAATGCGAC of *PROS*. The amiRNA were sequenced and cloned in the binary vector pCAMBIA1300, where the *Nos*-terminator sequence was previously cloned between the sites KpnI and SmaI. For the analysis of *PROS* expression, a fragment consisting of the 1246 base pairs upstream the *PROS* coding region was amplified from genomic DNA and cloned into the pCAMBIA 1381 vector which already contains the *GUS* reporter gene. *Agrobacterium tumefaciens* strain GV3101 was transformed with the resulting vectors and used to transform *Arabidopsis thaliana* (Col-0) by floral dip.

GUS Staining—For histochemical localization of β-glucuronidase (GUS) activity, tissues were vacuum-infiltrated with 50 mM Na-phosphate buffer pH 7.0 containing 0.5 mM potassium ferrocyanide, 0.5 mM potassium ferricyanide, 0.5% Triton X-100, 0.1% Tween-20, 10 mM Na_2-EDTA, and 2 mM 5-bromo-4-chloro-3-indolyl-β-D-glucuronic acid sodium salt (X-Gluc) (Phytotechnology Laboratories). Incubations were performed in the dark at 37 °C for 15 h. Tissues were clarified with ethanol: acetic acid (3:1), washed in 70% ethanol, and visualized using a stereoscopic microscope (Nikon SMZ800), and imaged with a Nikon Coolpix 4500 CCD digital camera.

RNA Extraction, RT, and Quantitative PCR—RNA was isolated from 21-day-old plants using TRIzol reagent (Invitrogen) following the manufacturer instructions. 500 ng of total RNA was reversely transcribed to the first strand of the cDNA using AMV transcriptase (Promega) and oligo-dT primers in a 20 μl volume reaction. A 1/100 dilution was used as a template in reactions for *PROS*, *ARC12*, and *UBC9*. A 1/10 dilution was used as a template in reactions for *CYP71A13* and *bHLH131*. The SYBR GREEN PCR Master Mix (Applied Biosystems) was used for amplification and detection of transcripts in an ABI prism 7300 thermocycler. The data were analyzed using the LinRegPCR quantitative PCR data analysis program (version 12.4). Primers used for quantitative PCR analysis of transcripts are: GATCCGTCTCCGTCTTCTGA and TCATCGCTATCGCAATTCTG for *PROS*; CATCTTGAAGGAGCAGTGGAG and GGGTTTGGATCCGTTAACAA for *UBC9*; ATCACCACCGTAATCGCCTCTC and TGAATCCCGTGAAATCAACCTTGG for *ARC12*; GTGCTTCGGTTGCATCCTTCTC and CGCCCAAGCATTGATTATCACCTC for *CYP71A13;* and GAAAGCAAAGGCGGTGAGAG and CAAGGCACACTTGGTTCTTCC for *bHLH131*.

Electron Microscopy—Fresh, unfixed, 41-day-old leaves of WT and *PROS* knock-down lines A and B were imaged in an Environmental Scanning Electron Microscope (ESEM) FEI Quanta 200 in environmental mode.

Morphometric Analysis of Pavement Cells—Fourth rosette leaves from 30-day-old plants were harvested from each genotype and fixed in 70% ethanol. Leaves were stained with a 10 μg/ml propidium iodide (MP Biochemicals) solution and imaged in a Zeiss LSM 510 META confocal laser scanning microscope using a 20x NA0.75 objective. Propidium iodide was excited with an HeNe laser at 543 nm, 19% of intensity, and the emission was collected using a LP 560 filter and a pinhole opening equivalent to 1 Airy unit. Whole leaves were imaged on an Epson Perfection 4870 PHOTO flatbed scanner for subsequent measurement of total leaf blade area. Adaxial pavement cells at the mid-third of the leaves were traced and measured with the aid of Fiji (28). The number of pavement cells at the adaxial epidermis for each leaf was extrapolated from the measurements of pavement cell area and leaf blade area for each leaf. Eight leaves and 100–200 pavement cells were measured for each genotype.

Accession Numbers—Sequence data from this article can be found in the GenBank™/EMBL databases under the following accession numbers: *PROS* (At4g24370); *SKD1* (At2g2760); *VPS60.1* (At3g10640); *IST1* (At1g34220); *CHMP1A* (At1g73030); *UBC9* (At4g27960); *LIP5* (At4g26750), *ARC12* (At1g69390), *CYP71A13* (At2g30770), *bHLH* (AT4G38070).

RESULTS

PROS (POSITIVE REGULATOR OF SKD1) Is a Plant-specific Protein That Interacts with SKD1 and LIP5—In a previous yeast two-hybrid (Y2H) screen using *Arabidopsis* SKD1 as bait (20), we identified AT4G24370 as a putative SKD1-interacting protein and named it PROS, for POSITIVE REGULATOR OF SKD1. The *PROS* coding region predicts a soluble protein of 164 amino acids, a molecular mass of 18.4 kDa, and two putative coiled coils domains (Fig. 1). Bioinformatics analysis with InterProScan did not predict the presence of any known functional domain. BLAST searches with the PROS protein sequence did not retrieve any previously identified ESCRT component in plants or in any other organisms. In addition, we were able to identify single copies of PROS-like sequences only in flowering plants (Fig. 1*A*).

PROS was confirmed to interact with *Arabidopsis* SKD1 in a directed Y2H (Fig. 1*B*) and *in vitro* pull-down assays using recombinant His-SKD1 and gluthatione-*S*-transferase (GST)-PROS (Fig. 1*C*). To test whether PROS interacts with endogenous SKD1, we incubated total protein extracts from *Arabidopsis* leaves with GST and GST-PROS. GST-PROS but not GST

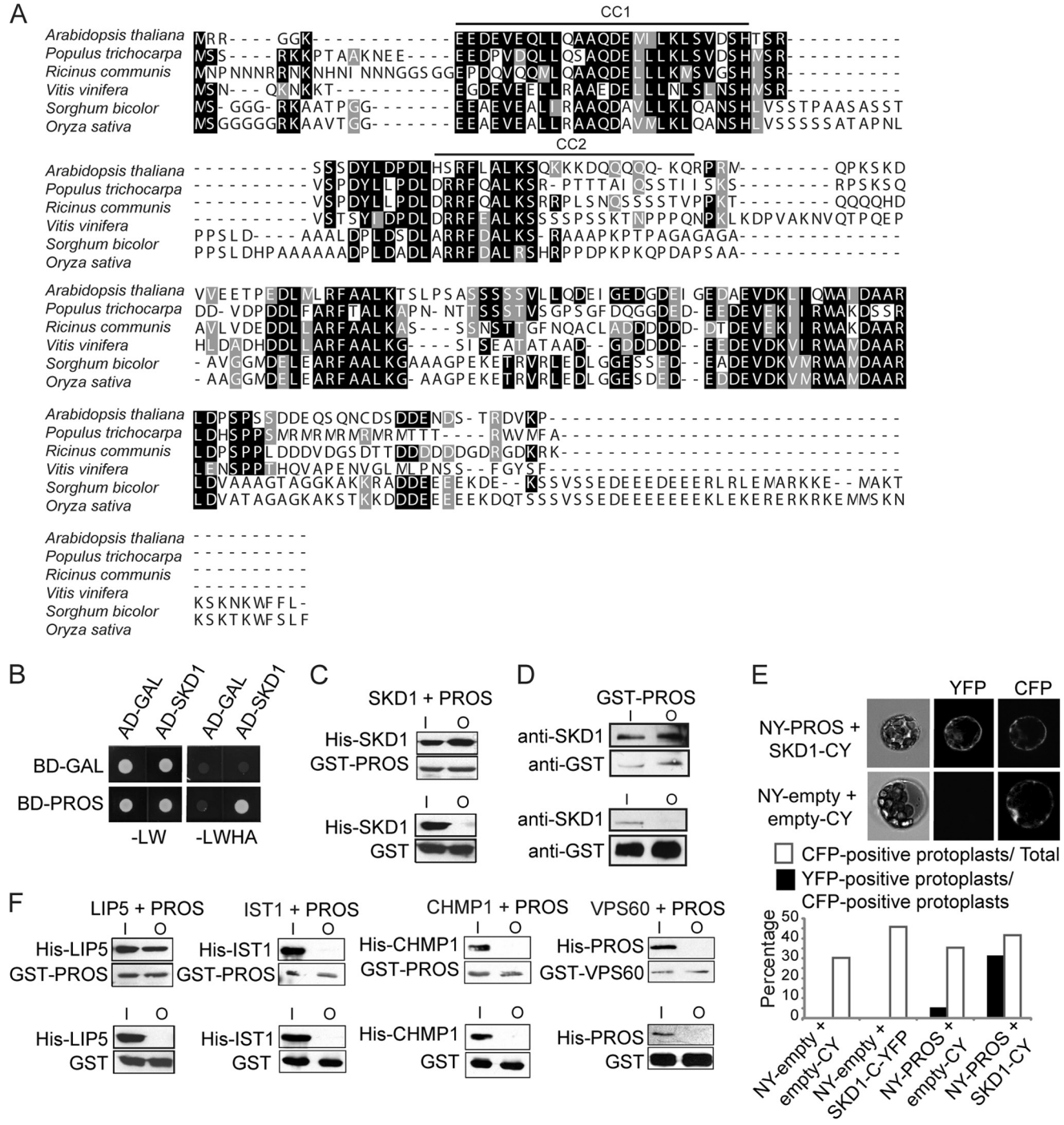

FIGURE 1. **PROS is a plant specific ESCRT component.** *A*, amino acid sequence alignment of PROS-like proteins in flowering plants. *Black* indicates identical residues, and *gray* represents similar residues. The position of the two predicted coiled coils (CC1 and CC2) is also indicated. *A. thaliana* PROS is 49% identical (64% similar) to the castor bean (*Ricinus communis*) homolog (XP_002513129) and 37% identical (50% similar) to the rice (*Oryza sativa*) homolog (Os08g0151500). *B*, Y2H analysis of AD-SKD1 with BD-PROS. Transformed cells were spotted on SD-LW or SD-LWHA plates to test for auxotrophic growth. *C*, *in vitro* pull-down assays of recombinant *Arabidopsis* SKD1 and PROS proteins tagged either with GST or His_6 and expressed in bacteria. *D*, pull-down assay of native SKD1 using recombinant GST-PROS and total protein extracts from *Arabidopsis* leaves. GST-PROS interacts with native *Arabidopsis* SKD1. *E*, BiFC assay on *Arabidopsis* protoplasts. A vector containing a ^{35}*Sprom::CFP* (pAVA574) reporter was co-transfected to assess transfection efficiency. Between 280 and 580 protoplasts were scored for each combination of vectors. *F*, *in vitro* pull down assays of recombinant PROS and several ESCRT proteins tagged with either GST or His_6 and expressed in bacteria. Recombinant PROS protein interacts with LIP5 but not with IST1, CHMP1, or VPS60. In all pull-down experiments, GST-tagged proteins bound to beads were incubated for 2 h with either His-tagged proteins or total leaf protein extracts (I, input). Beads were washed three times (O, out). Input and output fractions were loaded on an SDS-PAGE gel and transferred to a nitrocellulose membrane. Proteins were detected with specific antibodies anti-GST or anti-His_6.

alone was able to pull-down endogenous *Arabidopsis* SKD1 (Fig. 1*D*). In addition, the co-expression in *Arabidopsis* protoplasts of PROS fused to the N-terminal portion of YFP and SKD1 fused to the C terminus of YFP was able to reconstitute YFP fluorescence above background levels in a BiFC assay (Fig. 1*E*), indicating that the two proteins are able to interact *in vivo*.

By *in vitro* pull-down of recombinant proteins, we also found that PROS interacted with His-LIP5 but not with the accessory

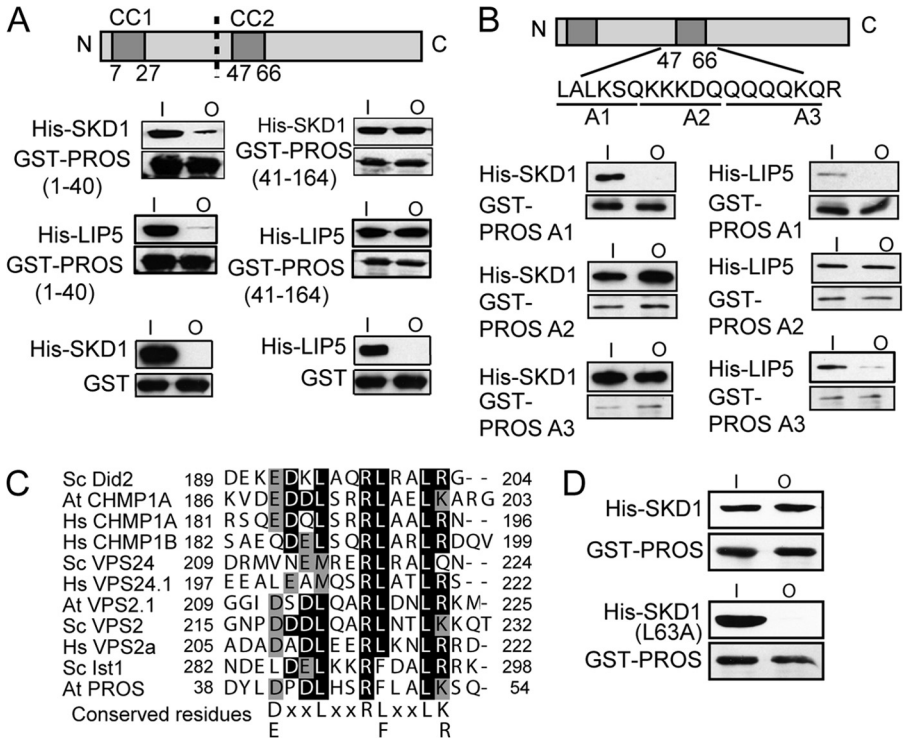

FIGURE 2. **PROS contains an internal MIM domain.** *A*, *in vitro* pull down of recombinant His-SKD1 and two fragments containing amino acids 1–40 and 41–164 of PROS fused to GST. *B*, *in vitro* pull-down of His-SKD1 and mutated GST-PROS proteins in which alanine substitutions were introduced in the first six positions (GST-PRO A1), in the second six positions (GST-PRO A2), or in the third six positions (GST-PROS A3) of the second coiled coil in PROS. *C*, diagram of PROS protein indicating the position of the putative MIM and amino acid sequence alignment of MIM domains in PROS and ESCRT-III proteins from *S. cerevisiae* (Sc), humans (Hs), and *A. thaliana* (At). *D*, *in vitro* pull-down of His-SKD1 with or without a L63A mutation in its MIT domain and GST-PROS. In all pull-down experiments, GST-tagged proteins bound to beads were incubated for 2 h with either His-tagged proteins or total leaf protein extracts (I, input). Beads were washed three times (O, out). Input and output fractions were loaded on an SDS-PAGE gel and transferred to a nitrocellulose membrane. Proteins were detected with specific antibodies anti-GST or anti-His_6.

ESCRT-III components His-CHMP1A, His-IST1, or His-VPS60.1 (Fig. 1*F*).

PROS Contains a Functional Internal MIM Domain—By performing *in vitro* pull down assays of truncated PROS proteins, we determined that the region between amino acid residues 41–164 containing the second coiled coil interacted with both His-SKD1 and His-LIP5 whereas the PROS N-terminal fragment (residues 1 to 40) showed only barely detectable interaction with either His-SKD1 or His-LIP5 (Fig. 2*A*). We introduced simultaneously six alanine substitutions along the 18 amino acid residues predicted to be part of the coiled coil (Fig. 2*B*) and found that mutations in the first six residues disrupted the interactions with both His-SKD1 and His-LIP5 (Fig. 2*B*). A closer examination of the second coiled coil region revealed the presence of a putative MIM (MIT-interacting motif) domain between amino acid residues 38 and 54 (Fig. 2*C*). Most MIM domains in core ESCRT-III subunits are located at the C-terminal region, which is known to autoinhibit the assembly of the ESCRT-III complex and to maintain the soluble monomeric pool in closed state (30, 31). Upon association with the endosomal membrane, ESCRT-III subunits change their conformation to an "open state" and their MIM domains become available for interactions with MIT (microtubule interacting and transport) domains such as the ones present in SKD1 and LIP5 (32, 33). To test whether the SKD1 MIT domain is required for interaction with PROS, we introduced a change in a conserved leucine residue (Leu-63 in *Arabidopsis* SKD1) known to be required for the interaction between yeast Vps4p and the Vps2p MIM domain (33). The recombinant His-SKD1(L63A) protein failed to interact with GST-PROS (Fig. 2*D*), indicating that the SKD1 MIT domain is necessary for interaction with PROS.

PROS Increases the in Vitro ATPase Activity of Arabidopsis SKD1 and Yeast Vps4p—To determine the effects of PROS on the enzymatic activity of SKD1, we used recombinant His-SKD1 in the presence or absence of PROS and other SKD1-interacting proteins in a colorimetric *in vitro* ATPase assay (Fig. 3). At equimolar concentrations, His-LIP5 and His-PROS caused ~1.2- and ~1.5-fold increase, respectively, in SKD1 ATPase activity (Fig. 3*A*). In yeast, Vta1p/LIP5 acts as a positive regulator of Vps4p by interacting through the Vps4p C-terminal domain and stimulating its oligomerization (23, 34). However, the interaction between the MIT domain of human VPS4 and the MIM domain of ESCRT-III proteins can directly stimulate VPS4 ATPase activity (35). To test whether the increase in SKD1 ATPase activity by PROS is comparable to that caused by other *Arabidopsis* ESCRT-III proteins, we used His-CHMP1A, which interacts with SKD1 and contains a C-terminal MIM (19). The addition of His-CHMP1A to His-SKD1 caused a ~1.3 increase in P_i release (Fig. 3*A*). However, because ESCRT-III proteins in solution tend to adopt a closed conformation with their MIM domains hidden between the N-terminal α-helices, it is possible that only a small fraction of the His-CHMP1 molecules in our assay were in an open conformation and able to bind SKD1. In fact, isolated MIM domain fragments have been

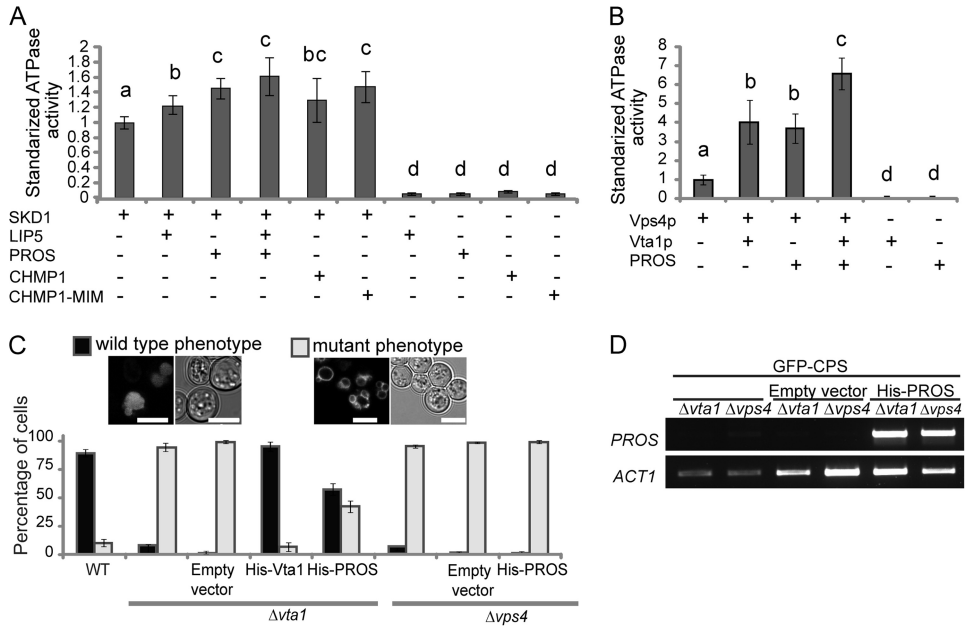

FIGURE 3. **PROS increases *in vitro* SKD1 and Vps4p ATPase activity.** *A*, *in vitro* ATPase activity of SKD1 alone or in combination with equimolar concentrations of LIP5, PROS, CHMP1, and a peptide containing the MIM of CHMP1 (CHMP1 109–203). *B*, *in vitro* ATPase assays of Vps4p with Vta1p and PROS. In both *A* and *B*, recombinant proteins expressed in bacteria were purified and used in a malachite green-based assay to measure P_i released from ATP. Bars represent standardized average values ($n = 8$) from two independent experiments. *Letters* above the bars represent statistical significance (one-way ANOVA followed by Tukey, $p < 0.05$); bars sharing a letter are not significantly different from one another. Error bars represent S.D. *C*, expression of His-PROS in Δ*vta1* but not in Δ*vps4* mutant strains is able to partially rescue the mis-sorting of the ESCRT cargo GFP-CPS. Δ*vta1* and Δ*vps4* mutant expressing GFP-CPS were transformed with empty plasmids, with *His-Vta1*, or *His-PROS*. Cells showing GFP signal in the vacuolar lumen were scored as "wild type phenotype" and those showing GFP signal on the vacuolar membrane, as "mutant phenotype". At least 100 cells for each genotype were analyzed. Scale bar, 5 μm. *D*, RT-PCR of *PROS* transcripts in the yeast strains used in *C*.

shown to have a much stronger positive effect on human VPS4 ATPase activity than whole-length ESCRT-III proteins (35). Consistently, when we added a C-terminal CHMP1 fragment containing the CHMP1 MIM domain plus 72 amino acid residues of the upstream sequence (His-CHMP1 109–203) to His-SKD1, we observed a ~1.5-fold increase in ATP hydrolysis (Fig. 3*A*), more similar to the activity increase caused by PROS. This is consistent with PROS having a constitutively exposed MIM domain. We also performed a similar *in vitro* ATPase assay using recombinant His-Vps4p from yeast and found that *Arabidopsis* PROS was also able to increase the activity of yeast Vps4p by ~4-fold (Fig. 3*B*).

Expression of PROS in Δvta1 Yeast Mutant Cells Partially Rescues MVB Sorting Defects—Although PROS is able to increase the *in vitro* ATPase activity of SKD1, it seems to act differently from the best characterized yeast Vps4p-positive regulator Vta1p. Whereas the C-terminal domain of yeast Vta1p binds the C-terminal domain of Vps4p promoting Vps4p oligomerization and stabilizing the Vps4p-Vta1p complex (23, 36), an internal MIM in PROS binds the MIT domain of SKD1. Nevertheless, we asked whether the expression of *Arabidopsis* PROS could alleviate endosomal sorting defects in a yeast Δ*vta1* mutant strain that mis-sorts GFP-CPS, an MVB cargo marker, to the vacuolar membrane (23). We scored the number of cells showing normal GFP-CPS distribution in the vacuolar lumen and those showing mis-sorting of GFP-CPS to the vacuolar membrane (Fig. 3*C*) in WT, Δ*vta1* cells, and also in Δ*vta1* cells transformed with vectors expressing His-Vta1p, His-PROS, or with an empty vector (Fig. 3*C*). The expression of His-Vta1p restored the normal sorting of GFP-CPS in almost 100% of the Δ*vta1* mutant cells, whereas the expression of PROS led to normal GFP-CPS localization in 60% of the cells. To determine whether PROS restores GFP-CPS localization in Δ*vta1* cells through a Vps4p-dependent mechanism, we expressed His-PROS in Δ*vps4* cells. PROS did not rescue the mis-sorting of GFP-CPS in this case, indicating that PROS requires Vps4p to partially restore the MVB sorting functions in the Δ*vta1* mutant (Fig. 3*C*). The expression of the *His-PROS* transgene in yeast cells was confirmed by RT-PCR (Fig. 3*D*).

PROS Knock-down Plants Are Dwarf and Show Cell Expansion Defects—To analyze the expression pattern of *PROS* in plants we cloned a fragment containing 1246 bp upstream the *PROS* coding sequence fused to the GUS and expressed it in WT Col-0 plants. The analysis of the resulting transgenic lines showed that *PROS* is ubiquitously expressed in leaves, roots, and in stamens and petals of flowers (Fig. 4).

We were unable to identify T-DNA lines with altered levels of *PROS* transcripts. Therefore, to elucidate the function of *PROS* in plants, we designed two artificial microRNAs (amiRNA A and B) (Fig. 5*A*). We analyzed ~80 independently transformed plants expressing either amiRNA A or B and identified plants with ~60%, and ~30% reduction in *PROS* transcript levels, respectively, compared with WT plants (Fig. 5, *A* and *B*). According to the Web microRNA designer tool (WMD2), there are no predicted off target genes for amiRNA A whereas there are two for amiRNA B, a putative cytochrome P450 (*CYP71A13*) and *ACCUMULATION AND REPLICATION OF CHLOROPLASTS 12* (*ARC12*), a gene coding for a protein involved in plastid division. Whereas we found no statistically significant differences in the *ARC12* transcript levels,

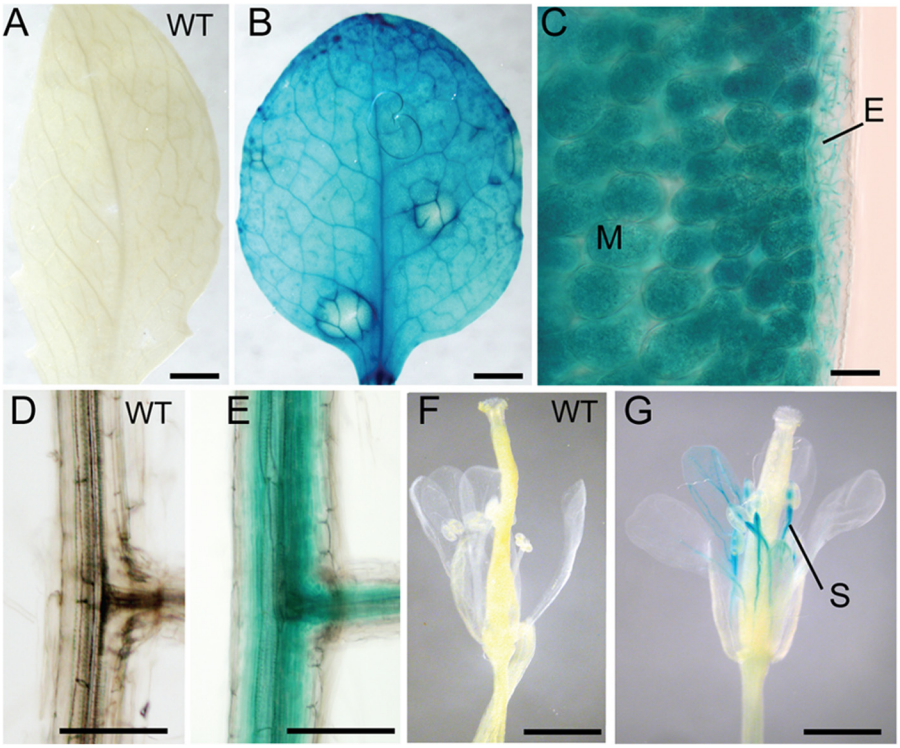

FIGURE 4. **Analysis of *PROS* expression.** Histochemical GUS detection in *Arabidopsis* plants transformed with a construct containing 1246 bp upstream the *PROS* coding sequence fused to the *GUS* gene. GUS activity was detected in all cell types of transgenic leaves (*A–C*), roots (*D*, *E*), and stamens, petals, and pedicels of flowers (*F*, *G*). *E*, epidermis; *M*, mesophyll, *S*, stamen. Scale bars, 1 mm (*A*, *B*, *F*, *G*), 200 μm (*C–E*).

CYP71A13 was strongly up-regulated not only in the amiRNA B lines but also in the amiRNA A plants (Fig. 5*B*). Since *CYP71A13* is involved in conferring resistance to fungal pathogens (37) and it is up-regulated under both biotic and abiotic stress conditions, the increased levels of *CYP71A13* transcripts in both amiRNA A and B plants is likely a indirect effect due to the silencing of *PROS*. Consistent with our gene expression analysis (Fig. 4), plants expressing *PROS* amiRNAs showed general morphological defects in all organs. *PROS* knock-down plants were dwarf, with wrinkled rosette leaves, and twisted inflorescence stems (Fig. 5, *C–J*). Their flowers had all floral parts in normal position and number but did not fully complete expansion (Fig. 5, *G* and *J*). On *PROS* knock-down rosette leaves, we observed regions of abnormally small pavement cells with reduced interdigitation compared with WT leaves (Fig. 5, *K–L*). In addition, trichomes with normal numbers of branches (3–4) but half the size of WT trichomes (Fig. 5, *M* and *N*) were common in these regions. To determine whether the reduction in leaf size was solely due to smaller leaf cells or to an additional reduction in cell number, we estimated the number of adaxial pavement cells per leaf blade of 30-day-old *PROS* knock-down plants and found it not to be different from WT controls (Fig. 4, *O–Q*), indicating that defective cell expansion is the main underlying cause for reduced leaf blade size.

DISCUSSION

ESCRT components were originally identified for their participation in MVB sorting but they are now known to control many other cellular functions such as cytokinesis, autophagy, cell polarity, and migration, miRNA activity, and mRNA transport (38). Consistently, when their ESCRT machinery is not functional, multicellular organisms show very strong and pleiotropic developmental defects that often lead to lethality. Many of these prominent developmental defects in ESCRT mutants can be correlated to alterations in receptor-mediated signaling due to MVB sorting defects. The most general defect is signaling up-regulation due to improper receptor sorting and degradation. However, mutations in different ESCRT components do not lead to identical developmental and signaling defects, and a current major challenge is to understand how the ESCRT machinery interacts with different signaling pathways, in specific cellular and developmental contexts, and in different organisms.

Like other ESCRT-III proteins, PROS contains an MIM domain that mediates its interaction with SKD1. ESCRT-III subunits are assumed to cycle between a closed, inactive, monomeric state in the cytoplasm and open, active, oligomeric state when associated with endosomal membranes (30, 31, 39). The MIM domains located at the C terminus of ESCRT-III subunits such as CHMP1 and VPS2 only become available for interactions with SKD1/VPS4 when the proteins are in open conformation. The fact that whole length PROS and a fragment containing the MIM domain of CHMP1 increase the *in vitro* SKD1 ATPase activity at comparable levels, suggests that the internal MIM domain of PROS may be constitutively exposed. Although we do not know whether PROS is part of the SKD1-LIP5 complex in plants, the fact that PROS can partially suppress MVB sorting defects in the yeast Δ*vta1*

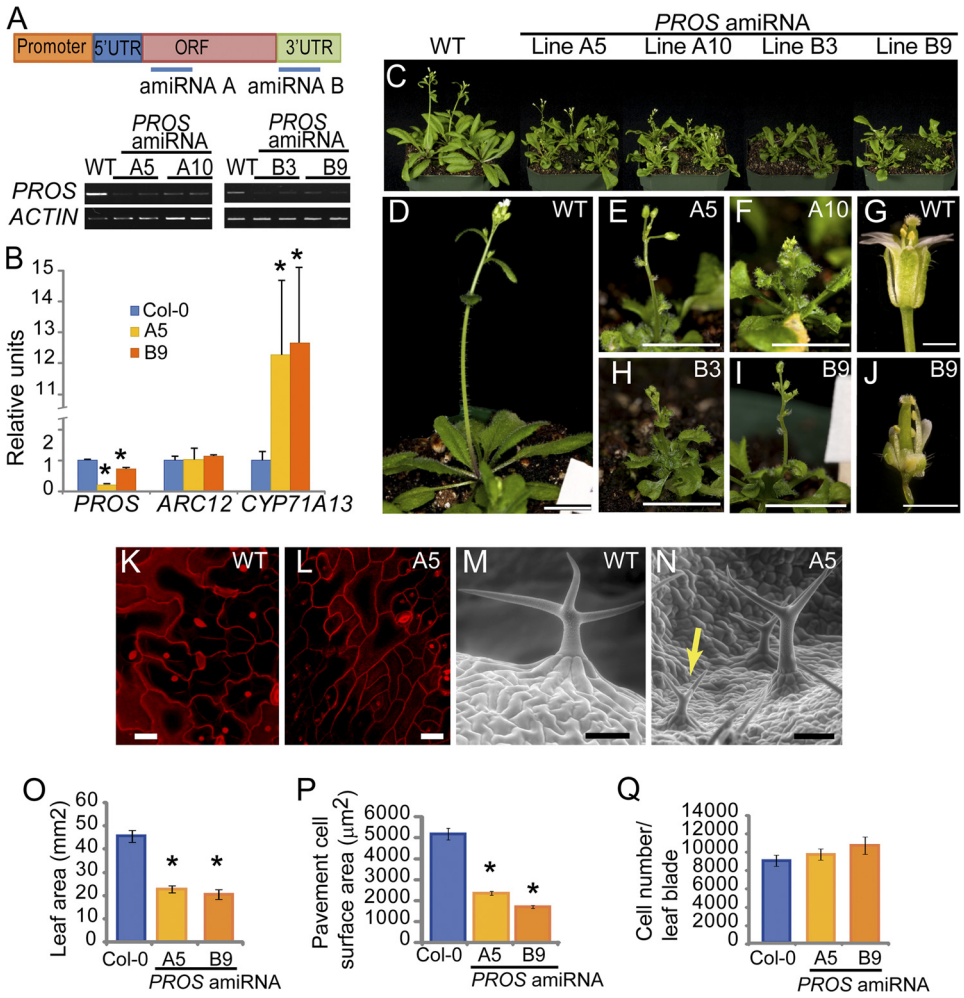

FIGURE 5. **Silencing of *PROS* in *Arabidopsis*.** *A*, two independent amiRNAs were designed to target the coding region (amiRNA A) and the 3′-UTR (amiRNA B). Expression of either amiRNA A (lines A5 and A10) or B (lines B3 and B9) resulted in a decrease of *PROS* transcript levels as shown by RT-PCR. Amplification of *ACTIN1* was used as control. *B*, qPCR shows a decrease *PROS* levels in plants expressing amiRNA A (line A5) and B (line B9) but no significant changes in the transcript levels of *ARC12*, a possible off target gene of amiRNA B. The expression of *PROS* and *ARC12* was normalized to *UBC9* (*UBIQUITIN-CONJUGATING ENZYME 9*). *CYP71A13*, another possible off target gene of amiRNA B was strongly up-regulated in both amiRNAA and B lines. The expression of *CYP71A13* was normalized to *bHLH131*. Bar graph represents average and error bars represent S.E. The *asterisks* indicate a significant difference compared with WT by Student's *t* test ($p < 0.05$). *C*, overview of 30-day-old WT Col-0 and plants expressing *PROS* amiRNA A (lines A5 and A10) or amiRNA B (lines B3 and B9). *D–J*, growth defects in 32-day-old *PROS* knock-down plants. *K–L*,confocal micrographs of adaxial rosette leaf epidermis stained with propidium iodide from 41-day-old WT (*K*) and *PROS* knock-down line A5 (*L*) plants. *M–N*, scanning electron micrographs of adaxial epidermis of rosette leaves from 41-day-old WT (*M*) and *PROS* knock-down line A5 (*N*). Note the underdeveloped trichomes in the *PROS* knock-down leaf (*arrow*), *O–Q*, quantification of the leaf blade area (*O*), pavement cell area in adaxial leaf epidermis (*P*), and estimated number of adaxial pavement cells per leaf blade (*Q*) in WT Col-0 and *PROS* knock-down lines. The fourth rosette leaf was used for all quantifications. Graphs represent data from 8 leaves and 100–200 pavement cells measured for each genotype. Bar graph represents average, and error bars represent S.E. The *asterisks* indicate a significant difference compared with WT by two-tailed Student's *t* test ($p < 0.05$). Scale bars, 1 cm (*D–J*), 20 μm (*K*, *L*), 100 μm (*M*, *N*).

mutant suggests that it can work as a positive regulator of SKD1/VPS4 *in vivo*.

The cell expansion and growth defects seen in PROS knock-down lines are consistent with defects in endosomal trafficking (40). However, we cannot exclude the possibility that PROS plays other ESCRT-independent functions in plants that affect cell and organ expansion.

In conclusion, we have identified a novel ESCRT component that seems to have evolved within the plant lineage. Its presence in plants but not in other organism is a clear indications of the almost unexplored variations of ESCRT functions across eukaryotes and the multiple regulatory mechanisms that control MVB sorting and the vacuolar degradation of plasma membrane proteins.

Acknowledgment—We thank David Katzmann (Mayo Clinic-Minnesota) for providing the yeast strains used in this study.

REFERENCES

1. Elia, N., Sougrat, R., Spurlin, T. A., Hurley, J. H., and Lippincott-Schwartz, J. (2011) Dynamics of endosomal sorting complex required for transport (ESCRT) machinery during cytokinesis and its role in abscission. *Proc. Natl. Acad. Sci. U.S.A.* **108,** 4846–4851
2. Guizetti, J., Schermelleh, L., Mäntler, J., Maar, S., Poser, I., Leonhardt, H., Müller-Reichert, T., and Gerlich, D. W. (2011) Cortical constriction during abscission involves helices of ESCRT-III–dependent filaments. *Science* **331,** 1616–1620
3. Wollert, T., Wunder, C., Lippincott-Schwartz, J., and Hurley, J. H. (2009) Membrane scission by the ESCRT-III complex. *Nature* **458,** 172–177

4. Fyfe, I., Schuh, A. L., Edwardson, J. M., and Audhya, A. (2011) Association of ESCRT-II with VPS20 generates a curvature sensitive protein complex capable of nucleating filaments of ESCRT-III. *J. Biol. Chem.* **286,** 34262–34270
5. Henne, W. M., Buchkovich, N. J., Zhao, Y., and Emr, S. D. (2012) The endosomal sorting complex ESCRT-II mediates the assembly and architecture of ESCRT-III Helices. *Cell* **151,** 356–371
6. Babst, M., Davies, B. A., and Katzmann, D. J. (2011) Regulation of Vps4 during MVB sorting and cytokinesis. *Traffic* **12,** 1298–1305
7. Nickerson, D. P., West, M., and Odorizzi, G. (2006) Did2 coordinates Vps4-mediated dissociation of ESCRT-III from endosomes. *J. Cell Biol.* **175,** 715–720
8. Stauffer, D. R., Howard, T. L., Nyun, T., and Hollenberg, S. M. (2001) CHMP1 is a novel nuclear matrix protein affecting chromatin structure and cell-cycle progression. *J. Cell Sci.* **114,** 2383–2393
9. Shim, J. H., Xiao, C., Hayden, M. S., Lee, K. Y., Trombetta, E. S., Pypaert, M., Nara, A., Yoshimori, T., Wilm, B., Erdjument-Bromage, H., Tempst, P., Hogan, B. L., Mellman, I., and Ghosh, S. (2006) CHMP5 is essential for late endosome function and down-regulation of receptor signaling during mouse embryogenesis. *J. Cell Biol.* **172,** 1045–1056
10. Xiao, J. (2008) Structural basis of Vta1 function in the multivesicular body sorting pathway. *Dev. Cell* **14,** 37–49
11. Yang, Z., Vild, C., Ju, J., Zhang, X., Liu, J., Shen, J., Zhao, B., Lan, W., Gong, F., Liu, M., Cao, C., and Xu, Z. (2012) Structural basis of molecular recognition between ESCRT-III like protein Vps60 and AAA-ATPase regulator Vta1 in the multi-vesicular body pathway. *J. Biol. Chem.* **287,** 43899–43908
12. Dimaano, C., Jones, C. B., Hanono, A., Curtiss, M., and Babst, M. (2008) Ist1 regulates Vps4 localization and assembly. *Mol. Biol. Cell* **19,** 465–474
13. Rue, S. M., Mattei, S., Saksena, S., and Emr, S. D. (2008) Novel ist1-did2 complex functions at a late step in multivesicular body sorting. *Mol. Biol. Cell* **19,** 475–484
14. Ghazi-Tabatabai, S., Saksena, S., Short, J. M., Pobbati, A. V., Veprintsev, D. B., Crowther, R. A., Emr, S. D., Egelman, E. H., and Williams, R. L. (2008) Structure and disassembly of filaments formed by the ESCRT-III subunit Vps24. *Structure* **16,** 1345–1356
15. Leung, K. F., Dacks, J. B., and Field, M. C. (2008) Evolution of the multivesicular body ESCRT machinery; retention across the eukaryotic lineage. *Traffic* **9,** 1698–1716
16. Winter, V., and Hauser, M.-T. (2006) Exploring the ESCRTing machinery in eukaryotes. *Trends Plant Sci.* **11,** 115–123
17. Shahriari, M., Richter, K., Keshavaiah, C., Sabovljevic, A., Huelskamp, M., and Schellmann, S. (2011) The *Arabidopsis* ESCRT protein-protein interaction network. *Plant Mol. Biol.* **76,** 85–96
18. Shahriari, M., Keshavaiah, C., Scheuring, D., Sabovljevic, A., Pimpl, P., Häusler, R. E., Hülskamp, M., and Schellmann, S. (2010) The AAA-type ATPase AtSKD1 contributes to vacuolar maintenance of *Arabidopsis thaliana*. *Plant J.* **64,** 71–85
19. Spitzer, C., Reyes, F. C., Buono, R., Sliwinski, M. K., Haas, T. J., and Otegui, M. S. (2009) The ESCRT-related CHMP1A and B proteins mediate multivesicular body sorting of auxin carriers in *Arabidopsis* and are required for plant development. *Plant Cell* **21,** 749–766
20. Haas, T. J., Sliwinski, M. K., Martínez, D. E., Preuss, M., Ebine, K., Ueda, T., Nielsen, E., Odorizzi, G., and Otegui, M. S. (2007) The *Arabidopsis* AAA ATPase SKD1 is involved in multivesicular endosome function and interacts with its positive regulator LYST-INTERACTING PROTEIN5. *Plant Cell* **19,** 1295–1312
21. Spitzer, C., Schellmann, S., Sabovljevic, A., Shahriari, M., Keshavaiah, C., Bechtold, N., Herzog, M., Müller, S., Hanisch, F. G., and Hulskamp, M. (2006) The *Arabidopsis elch* mutant reveals functions of an ESCRT component in cytokinesis. *Development* **133,** 4679–4689
22. Richardson, L. G. L., Howard, A. S. M., Khuu, N., Gidda, S. K., McCartney, A., Morphy, B. J., and Mullen, R. T. (2011) Protein-protein interaction network and subcellular localization of the *Arabidopsis thaliana* ESCRT machinery. *Frontiers Plant Sci.* **2,** 20
23. Azmi, I., Davies, B., Dimaano, C., Payne, J., Eckert, D., Babst, M., and Katzmann, D. J. (2006) Recycling of ESCRTs by the AAA-ATPase Vps4 is regulated by a conserved VSL region in Vta1. *J. Cell Biol.* **172,** 705–717
24. Babst, M., Sato, T. K., Banta, L. M., and Emr, S. D. (1997) Endosomal transport function in yeast requires a novel AAA-type ATPase, Vps4p. *EMBO J.* **16,** 1820–1831
25. Bracha-Drori, K., Shichrur, K., Katz, A., Oliva, M., Angelovici, R., Yalovsky, S., and Ohad, N. (2004) Detection of protein–protein interactions in plants using bimolecular fluorescence complementation. *Plant J.* **40,** 419–427
26. Yoo, S.-D., Cho, Y.-H., and Sheen, J. (2007) Arabidopsis mesophyll protoplasts: a versatile cell system for transient gene expression analysis. *Nature Protocols* **2,** 1565–1572
27. von Arnim, A. G., Deng, X. W., and Stacey, M. G. (1998) Cloning vectors for the expression of green fluorescent protein fusion proteins in transgenic plants. *Gene* **221,** 35–43
28. Schindelin, J., Arganda-Carreras, I., Frise, E., Kaynig, V., Longair, M., Pietzsch, T., Preibisch, S., Rueden, C., Saalfeld, S., Schmid, B., Tinevez, J. Y., White, D. J., Hartenstein, V., Eliceiri, K., Tomancak, P., and Cardona, A. (2012) Fiji: an open-source platform for biological-image analysis. *Nat Methods* **9,** 676–682
29. Schwab, R., Ossowski, S., Riester, M., Warthmann, N., and Weigel, D. (2006) Highly specific gene silencing by artificial microRNAs in *Arabidopsis*. *Plant Cell* **18,** 1121–1133
30. Shim, S., Kimpler, L. A., and Hanson, P. I. (2007) Structure/function analysis of four core ESCRT-III proteins reveals common regulatory role for extreme C-terminal domain. *Traffic* **8,** 1068–1079
31. Lata, S., Roessle, M., Solomons, J., Jamin, M., Gottlinger, H. G., Svergun, D. I., and Weissenhorn, W. (2008) Structural basis for autoinhibition of ESCRT-III CHMP3. *J. Mol. Biol.* **378,** 816–825
32. Skalicky, J. J., Arii, J., Wenzel, D. M., Stubblefield, W.-M. B., Katsuyama, A., Uter, N. T., Bajorek, M., Myszka, D. G., and Sundquist, W. I. (2012) Interactions of the human LIP5 regulatory protein with endosomal sorting complexes required for transport. *J. Biol. Chem.* **287,** 43910–43926
33. Obita, T., Saksena, S., Ghazi-Tabatabai, S., Gill, D. J., Perisic, O., Emr, S. D., and Williams, R. L. (2007) Structural basis for selective recognition of ESCRT-III by the AAA ATPase Vps4. *Nature* **449,** 735–739
34. Azmi, I. F., Davies, B. A., Xiao, J., Babst, M., Xu, Z., and Katzmann, D. J. (2008) ESCRT-III family members stimulate Vps4 ATPase activity directly or via Vta1. *Dev. Cell* **14,** 50–61
35. Merrill, S. A., and Hanson, P. I. (2010) Activation of human VPS4A by ESCRT-III proteins reveals ability of substrates to relieve enzyme autoinhibition. *J. Biol. Chem.* **285,** 35428–35438
36. Yang, D., and Hurley, J. H. (2010) Structural role of the Vps4-Vta1 interface in ESCRT-III recycling. *Structure* **18,** 976–984
37. Nafisi, M., Goregaoker, S., Botanga, C. J., Glawischnig, E., Olsen, C. E., Halkier, B. A., and Glazebrook, J. (2007) *Arabidopsis* cytochrome P450 monooxygenase 71A13 catalyzes the conversion of indole-3-acetaldoxime in camalexin synthesis. *Plant Cell* **19,** 2039–2052
38. Rusten, T. E., Vaccari, T., and Stenmark, H. (2012) Shaping development with ESCRTs. *Nat. Cell Biol.* **14,** 38–45
39. Zamborlini, A., Usami, Y., Radoshitzky, S. R., Popova, E., Palu, G., and Göttlinger, H. (2006) Release of autoinhibition converts ESCRT-III components into potent inhibitors of HIV-1 budding. *Proc. Natl. Acad. Sci. U.S.A.* **103,** 19140–19145
40. Katsiarimpa, A., Kalinowska, K., Anzenberger, F., Weis, C., Ostertag, M., Tsutsumi, C., Schwechheimer, C., Brunner, F., Hückelhoven, R., and Isono, E. (2013) The deubiquitinating enzyme AMSH1 and the ESCRT-III subunit VPS2.1 are required for autophagic degradation in *Arabidopsis*. *Plant Cell* **25,** 2236–2252